Spectral response of crystalline acetanilide and *N*-methylacetamide: Vibrational self-trapping in hydrogen-bonded crystals

Julian Edler* and Peter Hamm†
Universität Zürich, Physikalisch Chemisches Institut, Winterthurerstrasse 190, CH-8057 Zürich, Switzerland
(Received 12 February 2004; published 28 June 2004)

Femtosecond pump-probe and Fourier transform infrared spectroscopy is applied to compare the spectral response of the amide I band and the NH-stretching band of acetanilide (ACN) and *N*-methylacetamide (NMA), as well as their deuterated derivatives. Both molecules form hydrogen-bonded molecular crystals that are regarded to be model systems for polypeptides and proteins. The amide I bands of both ACN and NMA show a temperature-dependent sideband, while the NH bands are accompanied by a sequence of equidistantly spaced satellite peaks. These spectral anomalies are interpreted as a signature of vibrational self-trapping. Two different types of states can be identified in both crystals in the pump-probe signal: a delocalized free-exciton state and a set of localized self-trapped states. The phonons that mediate self-trapping in ACN and deuterated ACN are identified by their temperature dependence, confirming our previous results. The study shows that the substructure of the NH band in NMA (amide *A* and amide *B* bands) originates, at least partly, from vibrational self-trapping and not, as often assumed, from a Fermi resonance.

DOI: 10.1103/PhysRevB.69.214301 PACS number(s): 63.20.Pw, 63.20.Ry

I. INTRODUCTION

The α helix is one of the most common secondary structure motifs in proteins. The three-dimensional (3D) configuration of the α helix is stabilized by three quasi-one-dimensional chains of hydrogen bonds, which run through the helix and connect the C═O and N-H groups of the peptide units. It had been proposed many years ago that vibrational excitations of the amide groups in such a system could self-localize and play an important role in the energy transport of proteins.[1]

Self-localization or self-trapping of vibrational excitations is described by the polaron Hamiltonian, which combines two different coupling mechanisms:[2,3] (a) exciton coupling and (b) phonon coupling. Exciton coupling leads to delocalization of a vibrational excitation, caused by electrostatic interaction between the individual peptide units.[4,5] The vibrational excitation can either be the N-H or the C═O stretching vibration of the peptide unit (the latter is often referred to as the amide I mode). Analogous to electronic molecular excitons, the delocalized states are also called vibrational excitons or vibrons.

The vibrational excitons, in turn, are coupled to lattice phonons through an anharmonic (nonlinear) coupling term, which is mediated through the hydrogen bonds that stabilize the three-dimensional (3D) structure of the system. The exciton-phonon coupling has been rationalized as follows.[6] It is well known that the length of the hydrogen bond modulates the transition frequency of either the amide I or NH vibration mode of the peptide unit.[7] This interaction is responsible for a contraction of the hydrogen bond once one of the amide modes is vibrationally excited. As a consequence, the initially delocalized vibrational exciton collapses to form a self-localized state.

Hydrogen-bonded crystals, such as acetanilide (CH_3-CONH-C_6H_5, ACN) and N-methylacetamide (CH_3-CONH-CH_3, NMA), are commonly regarded as model systems for regular secondary protein structures. It had been recognized some time ago that the infrared absorption spectra of ACN exhibits anomalies in the regions of the amide I and NH-stretching modes.[8,9] The amide I mode consists of a single peak at 1666 cm^{-1} at room temperature. With decreasing temperatures, an additional peak appears at 1650 cm^{-1}. The NH mode, on the other hand, is weakly temperature dependent and consists of a main peak at 3295 cm^{-1}, accompanied by an almost regular series of satellite peaks towards lower frequencies. The origin of the unconventional amide I band has been the topic of many theoretical and experimental studies, including infrared spectroscopy, Raman scattering, x-ray scattering, and neutron scattering.[3,6,8,10–19] After carefully excluding more conventional explanations, Careri and co-workers have proposed that the spectral anomaly is related to vibrational self-trapping.[18]

In theoretical discussions of vibrational self-trapping, the exciton coupling is often neglected in a first step, since it is smaller than the exciton-phonon coupling, and included only afterwards in a perturbative manner.[3,6] The problem simplifies significantly when one further takes into account the one order of magnitude difference between the frequencies of the phonon modes and the high frequency vibrational mode, allowing an adiabatic "Born-Oppenheimer"-like separation of time scales. In this approximation, the high frequency vibration adopts adiabatically to the position of the phonon coordinates. As a result, the potential energy surface for each excitation level of high frequency mode is expressed as a function of phonon coordinates, as shown in Fig. 1. The nonlinear exciton-phonon coupling gives rise to a displacement of the potential energy surface of the self-trapped state. The minimum of that potential energy surface is shifted towards smaller intermolecular distances, giving rise to a stronger hydrogen bond in the excited sate. Consequently, a "Franck-Condon-like" progression is obtained for the absorption spectrum, consisting of one vibrational excitation plus several quanta of phonon excitation.

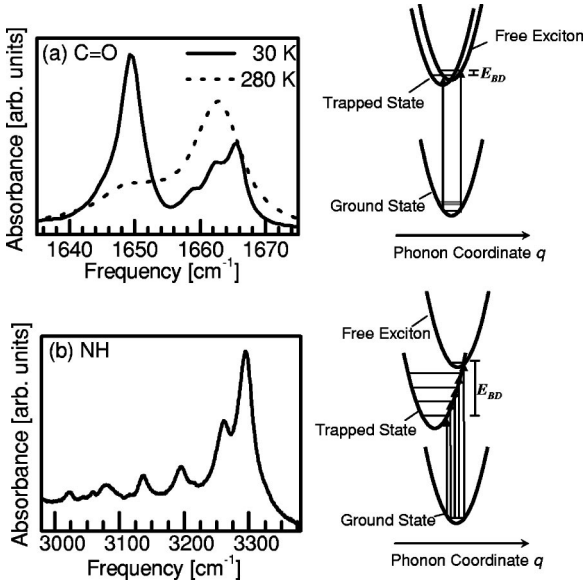

FIG. 1. (a) Absorption spectrum of the CO band of crystalline ACN, showing a temperature-dependent doublet. The peak at 1650 cm^{-1} corresponds to a self-trapped state and the one at 1666 cm^{-1} to a free exciton. (b) Absorption spectrum of the NH band, consisting of a main peak at 3295 cm^{-1} (free exciton) and a sequence of satellite peaks (self-trapped states). The proposed schemes of potential energy surfaces are depicted on the right-hand side. E_{BD} represents the binding energy of the self-trapped state.

When the displacement of ground- and excited-state potential energy surface is small (e.g., for the C═O band in ACN), only the zero-phonon transition (i.e., the 1650 cm^{-1} band) carries a noticeable oscillator strength at zero temperature and all other transitions are weak. With increasing temperatures, phonons in the C═O ground state are thermally excited, and the intensity of the zero-phonon line diminishes. The intensity is expected to decrease with temperature according to a $e^{-\gamma T^2}$ law, in perfect agreement with the experimentally observed dependence of the 1650 cm^{-1} band in ACN.[6,18,20] This agreement is presently considered to be the strongest evidence for self-trapping of the amide I band of ACN. In the case of the N-H mode, exciton-phonon coupling is significantly larger and the binding energy E_{BD} amounts to several phonon quanta. Therefore, one can observe a progression of self-trapped states in the NH band (see Fig. 1).

Recently, we performed femtosecond infrared pump-probe experiments, providing strong evidence for the self-trapping theory.[21–23] A study of the NH band revealed the phonons that couple to the NH mode and mediate self-trapping.[21] Moreover, we showed that the two amide I substates of ACN exhibit a distinctively different response on selective excitations, a result which has been interpreted in terms of the degree of delocalization of both states.[22] In addition, we were able to definitely exclude the possibility of a Fermi resonance and conformational substates as alternative explanations for the temperature dependence of the amide I mode,[23] confirming previous studies.[12,24]

Compelling evidence for vibrational self-trapping has so far only been gathered for crystalline ACN. However, the mechanism is expected to be generic, and should occur in any crystal with comparable structure. In particular, one expects to observe it in NMA, which is often regarded to be *the* model compound for peptides and proteins. Both crystals, ACN and NMA, have an orthorhombic structure and consist of quasi-one-dimensional chains of hydrogen-bonded peptide units (-CO-NH-) with structural properties that are similar to those of α helices.[25,26] Nevertheless, no convincing experimental evidence for self-trapping in NMA has been found so far. In the present study, we follow the strategy to transfer the knowledge we have gathered for ACN, for which vibrational self-trapping is clear and by now, well established, to NMA. To this end we compare the infrared absorption spectra and the pump-probe spectra of the amide I and NH mode of four different hydrogen-bonded crystals: ACN, deuterated ACN (CD_3-CONH-C_6D_5, ACN-D_8), NMA, and deuterated NMA (CD_3-CONH-CD_3, NMA-D_6). We will see that certain nonlinear spectroscopic fingerprints appear in comparable ways for both molecules, from which we conclude that the mechanism giving rise to the complex band shape of the NH and CO mode of both materials has the same origin.

II. MATERIALS AND METHODS

Femtosecond IR pump-probe experiments were performed with pulses with a bandwidth of 200 cm^{-1} full width at half maximum (FWHM), a pulse energy of 1–1.5 μJ, and a pulse duration of 150 fs at a 1 kHz repetition rate.[27] A small fraction of the infrared pulses was split off to obtain broadband probe and reference pulses, which were spectrally dispersed after interaction with the sample and detected with a 31-channel HgCdTe detector array (8 cm^{-1} resolution). The main part of the infrared pulses was used as pump pulses that were spectrally filtered for some of the experiments using an adjustable Fabry-Perot filter (bandwidth of 30 cm^{-1}), yielding a pump-pulse duration of 250 fs (FHWM). Infrared absorption spectra were measured on a BioRad FTS 175C spectrometer equipped with a highly sensitive mercury cadmium telluride (MCT) detector.

ACN (zone refined, purity 99.95%) and NMA (purity 99+%) were obtained from Aldrich, ACN-D_8 (98%) from Cambridge Isotope Laboratories, and NMA-D_6 (98.3%) from C/D/N isotopes. Monocrystalline ACN, NMA, and NMA-D_6 were prepared by cooling a thin layer of the molten substance between two CaF_2 windows. In the case of NMA, the sample was heated in a dry box to about 80°C beforehand in order to remove any possible water contaminations of the highly hygroscopic substance. Monocrystalline ACN-D_8 was grown out of a concentrated solution of ethanol/chloroform (20/80) on a CaF_2 window. For the experiments we carefully selected samples that showed only one crystalline orientation. The spectra were obtained with the *E* vector parallel and perpendicular to the hydrogen bond chain (in ACN the *b* and *c* axes, and in NMA the *a* and *c* axes). The comparison between spectra obtained with different polarizations confirmed that our samples were in a monocrystalline phase. In the cases of ACN and NMA-D_6 the crystals in the sample were perfectly aligned in one direction, while the ACN-D_8 and NMA samples showed some slight disorder. The samples were placed in a cryostat and

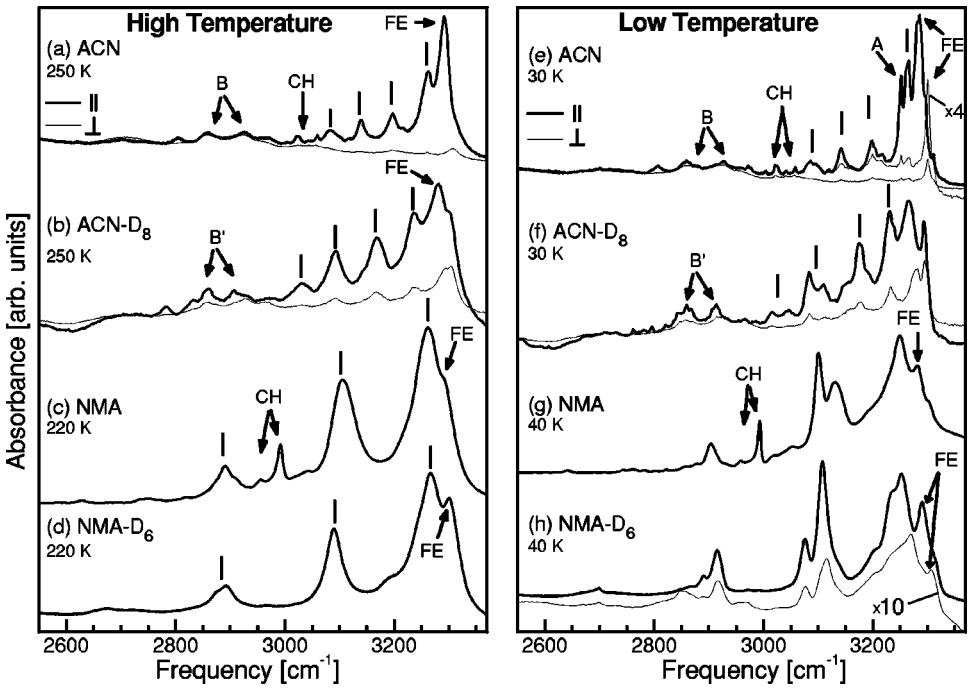

FIG. 2. IR spectrum of the NH band of ACN, ACN-D_8, NMA, and NMA-D_6 at high temperatures (a)–(d) and at low temperatures (e)–(h). All four crystals show similar band shapes, consisting of a main peak and a sequence of three to four satellite peaks. The CH modes, the amide I overtone (A) and the *B* modes are not part of the NH mode. The thick lines are for parallel polarization of the IR light with respect to the hydrogen-bonded chain and the thin lines for perpendicular polarization. For NMA-D_6 the perpendicular spectra are magnified by a factor of 10, for ACN by a factor of 4. The self-trapped states are marked by black bars and the free-exciton peak by FE.

experiments were performed at temperatures between 18 and 293 K. All spectra of NMA were measured at temperatures below the solid phase transition, which occurs between 274 and 283 K.[26,28]

III. EXPERIMENTAL RESULTS

A. Absorption spectra of the NH and the C═O bands

Figures 2(a)–2(h) show the absorption spectra in the spectral range of the NH mode of crystalline ACN, ACN-D_8, NMA, and NMA-D_6 at high (250 and 220 K) and low temperatures (≈30 K). Since the spectra are congested we will first discuss the contributions from other bands than the NH stretching band. We can identify CH stretching modes by comparing the C deuterated with the nondeuterated compounds. Figure 2 shows that the CH modes appear around 3000 cm^{-1} (ACN 3005, 3042, 3058, and 3118 cm^{-1}; NMA 2995 and 2993 cm^{-1}). Another peak, which is not part of the NH band, is labeled with "A" in the ACN spectrum [see Fig. 2(e)] and has been assigned previously to an overtone of the amide I mode.[10] All spectra show a strong polarization dependence and most bands are only observed when the *E* vector is oriented parallel to the NH groups.[9,29] Only the *B* and *B′* bands in the spectra of ACN and ACN-D_8 (ACN 2860 and 2925 cm^{-1}; ACN-D_8 2860 and 2913 cm^{-1}) show hardly any polarization dependence, and hence are attributed to overtone/combination modes of unknown origin.

If one combines the above observations and takes only the peaks that can be assigned to the NH band into account, one realizes that all four molecules exhibit an NH band which consists of a main band accompanied by a series of almost equidistant satellite peaks towards lower frequencies. The spacing between the four satellite peaks is ≈60 cm^{-1} for ACN and ≈70 cm^{-1} for ACN-D_8. In NMA, the separation between the satellite peaks is about three times larger. The satellite peaks in NMA and NMA-D_6 further split into doublets at low temperatures [Figs. 2(g) and 2(h)]. This splitting has been observed before and is of unclear origin.[30–32] In ACN the NH main peak at 3295 cm^{-1} is observed both in the parallel and perpendicular measurements, however, with a relative shift of 11 cm^{-1} [Fig. 2(a)]. The shift corresponds to the "Davydov" splitting and shows that the main peak in ACN is a delocalized state, i.e., a free-exciton state.[9]

Previous works have started from the assumption that the NH spectrum of ACN contains nine satellite peaks.[6,14,18,20,21] However, given the polarization dependence and the comparison with ACN-D_8, one must conclude that only the highest four satellite peaks are "real" (i.e., belong to the NH band), while the lower frequency part of the spectrum is perturbed by CH vibrations and weak overtones and/or combination modes.

Figures 3(a) and 3(b) show the absorption spectra of the amide I mode of ACN and NMA at different temperatures. As described before, an "anomalous" band appears at 1650 cm^{-1} in ACN with decreasing temperatures. The "nor-

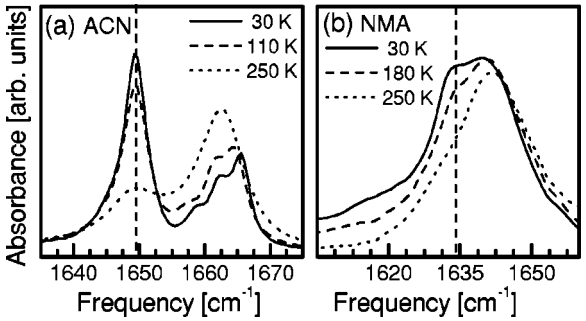

FIG. 3. IR spectrum of the amide I band of crystalline (a) ACN and (b) NMA at three different temperatures. The vertical line marks the position of the temperature-dependent sideband. The IR light was polarized parallel to the hydrogen-bonded chain.

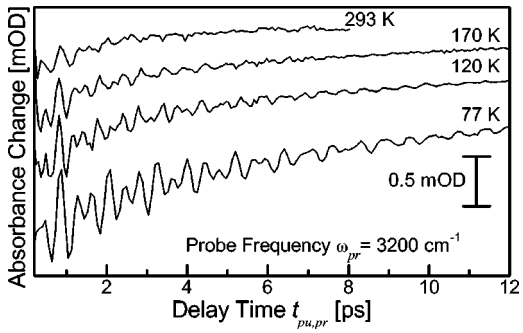

FIG. 4. The transient response of ACN after impulsive excitation for a probe frequency (3200 cm^{-1}) which coincides with one of the self-trapped states. The temperature is varied from 77 to 293 K.

mal" amide I band, on the other hand, splits into three subbands and decreases in intensity at low temperatures.[18,33] Interestingly, we also observe a temperature-dependent sideband in the amide I spectrum of NMA at 1634 cm^{-1}, whose separation from the main band, however, is about three times smaller than in ACN.

B. Impulsive excitation of the NH band

Crystalline ACN. In this section we use broadband pump pulses (bandwidth 200 cm^{-1}) to impulsively excite a section of the absorption spectrum, which includes the NH main peak and the first three satellite peaks. As a representative example, Fig. 4 shows the transient response for probe frequencies of 3200 cm^{-1}. The striking feature is strong oscillations, which at 77 K persist up to 14 ps. With increasing temperature, the oscillations decay faster and their amplitude decreases. A spectral analysis of the beating structure is obtained from the Fourier transformation

$$\Delta A(\omega,\omega_{pr}) = \int_0^\infty dt_{pu,pr} e^{iwt_{pu,pr}} \Delta A(t_{pu,pr},\omega_{pr}), \qquad (1)$$

where $\Delta A(t_{pu,pr},\omega_{pr})$ is the pump-probe signal (i.e., the transient response change plotted in Fig. 4) for delay times $t_{pu,pr}$ between pump and probe pulse at probe frequency ω_{pr}. The absolute value spectrum $|\Delta A(\omega,\omega_{pr})|$ is shown in Figs. 5(d) and 5(e) as a two-dimensional (2D) plot for 293 and 77 K. In this representation, the x axis corresponds to the probe frequency ω_{pr} and the y axis to the frequency ω, which is revealed by the Fourier transformation. The 2D plot at 77 K shows clearly two major frequency components at 54 and 83 cm^{-1}. The oscillations reach their maxima at probe frequencies which correspond to the peaks of the NH absorption band. Vertical cuts through the spectra at the position of the satellite peaks are shown in Figs. 5(c) and 5(f). A comparison between low and high temperature data reveals clearly that the frequencies of the two major oscillations decrease to 48 and 76 cm^{-1} at 293 K. In Fig. 6, the frequencies of the two major modes are plotted against temperature and compared with the frequencies of the phonon modes in the low frequency Raman spectrum (the latter taken from Johnston *et al.*[34]).

The impulsive excitation with an ultrafast laser pulse may result in the creation of vibrational wave packets, which give rise to oscillations in the pump-probe signal. Principally speaking, two different generation mechanisms of such wave packets are possible: (i) impulsive absorption, yielding a wave packet in the excited state, in which case the beating frequency should represent the energy separation between (coupled) states in the NH manifold of states, and (ii) a Raman-like process resulting in a ground-state wave packet, giving rise to phonon excitation. Impulsive absorption and Raman-like excitation are expected to occur simultaneously with probabilities that are given by the Franck-Condon factors of the individual transitions.

In Ref. 21, we have used two observations as an argument to assign the beatings in the pump-probe signal of ACN to a ground-state wave packet: (i) The lifetime of the excited state [400 fs, see Fig. 7(a)] is too short to support an excited state wave packet that persists for many picoseconds. This discrepancy becomes even more pronounced at low temperatures, where the coherence decay time increases significantly, while the excited state lifetime stays about the same [600 fs,

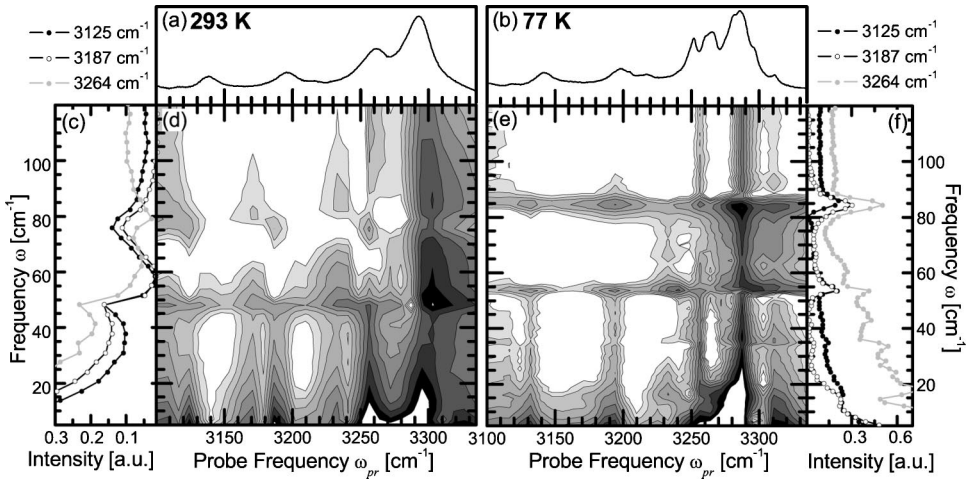

FIG. 5. (a) and (b) Absorption spectra of crystalline ACN, showing the NH band for 293 and 77 K. (d) and (e) The 2D plot of the absolute value of the Fourier transformation of the transient pump-probe signal after impulsive excitation. ω_{pr} is the frequency of the probe pulse and ω results from the Fourier transformation of the pump-probe signal with respect to delay time $t_{pu,pr}$ between pump and probe pulses. (c) and (f) Vertical cuts through the 2D spectrum at frequencies corresponding to the satellite peaks.

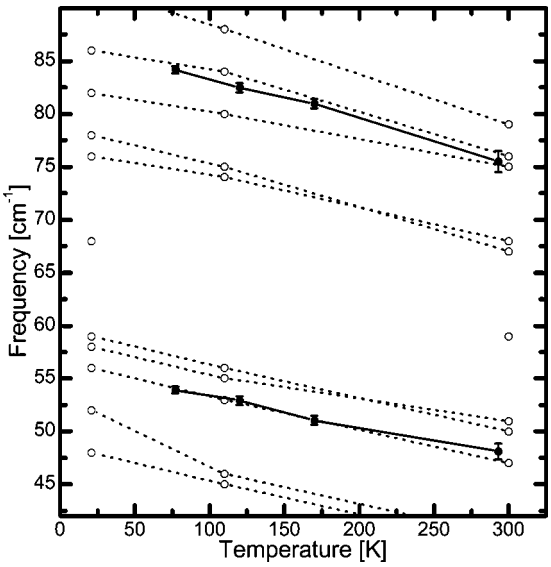

FIG. 6. Temperature dependence of the low-frequency Raman modes (◦) in ACN, taken from Johnston *et al.* (Ref. 34), and of the beating frequencies observed in the pump-probe experiment (•). The temperature dependence of the beating frequencies perfectly matches that of the Raman modes.

see Fig. 7(a)]. (ii) At room temperature, the frequency of the quantum beats does not fit the frequency spacings in the absorption spectrum. At lower temperatures, however, the beating frequency increases slightly and the absorption spectrum becomes more structured, so that the 54 cm^{-1} beating frequency in fact matches the frequency spacing between the 3198 (the second satellite peak) and the 3252 cm^{-1} bands (the first overtone of the amide I) at 77 K.

Nevertheless, our previous interpretation of a ground-state wave packet is validated by the temperature dependence of the beating frequency of the two major components (Fig. 6). In the case of a ground-state wave packet, the temperature dependence of the beating frequencies should match that of certain Raman modes. The low-frequency Raman spectrum of ACN has been the subject of several studies[18,34–36] and

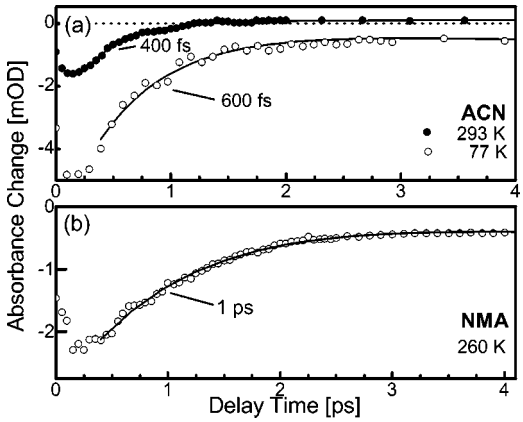

FIG. 7. The transient signal of ACN and NMA after selective excitation of the free-exciton peak. In the case of ACN the signal recovers on a 400 fs time scale at 293 K and on a 600 fs time scale at 77 K. In NMA the signal relaxes on a 1 ps time scale.

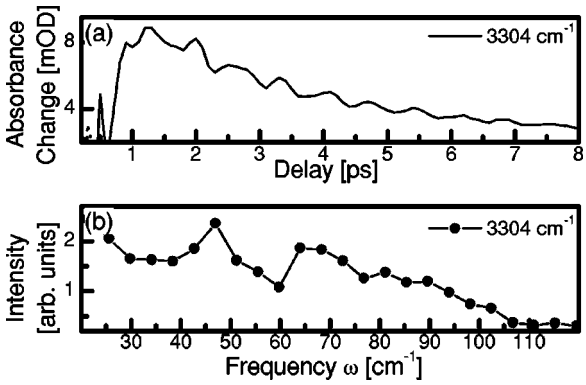

FIG. 8. (a) The transient signal of ACN-D_8 after impulsive excitation for a probe frequency which coincides with the free exciton, showing pronounced oscillations. (b) The Fourier-transform spectra show a sharp band at 47 cm^{-1} and a broadband at 80 cm^{-1}.

contains a total of 24 Raman active modes. In Fig. 6, we compare the temperature dependence of the beating frequency with that of the Raman-active phonons of the crystal and find an excellent agreement. Furthermore, the linewidth of the phonon modes narrows,[34] in agreement with the Fourier transform spectra in Figs. 5(c) and 5(f). Hence, we conclude that the beatings in the pump-probe signal reflect a coherent excitation of two distinct phonons in the NH ground state.

Interestingly, the pump-probe experiment selectively excites just 2 out of 24 Raman-active phonons. In the present experiment, the phonons are excited by a stimulated impulsive Raman process, which is resonantly enhanced by the NH absorption band. Such a process is only possible if the respective Raman modes are coupled to the NH excitation. In the representation of Fig. 1, such a coupling gives rise to a shift of the potential energy surfaces, i.e., it renders the phonon to be "Franck-Condon" active. In other words, the coupling observed in the pump-probe experiment is precisely the same as the one that is responsible for polaron formation. Combining these arguments, we conclude that the phonons we observe in the pump-probe experiment are indeed those phonons that mediate self-trapping.

Crystalline ACN-D_8. The transient signal in ACN-D_8 shows also a striking beating pattern (Fig. 8) similar to ACN. The Fourier transform spectrum contains clearly two frequency components: a sharp peak at 47 cm^{-1} and a broad peak at about 80 cm^{-1}. Since the molecular weight and crystal structure of ACN-D_8 are comparable to ACN, one indeed expects to excite the same phonons with similar frequencies. The comparison with the splittings in the absorption spectrum rules out an excited-state wave packet. Raman spectra of fully deuterated ACN show that the spectra below 60 cm^{-1} do not change much upon deuteration and contain a distinct mode at about 50 cm^{-1} and a broad band between 60 and 100 cm^{-1}.[37] Consequently, the oscillations are assigned to a ground-state wave packet, using the same arguments as in the previous paragraph. This is direct proof that the NH mode in ACN-D_8 is coupled to low frequency phonons and indicates that the multiplicity of the NH band in ACN-D_8 is caused by self-trapping, just as in ACN.

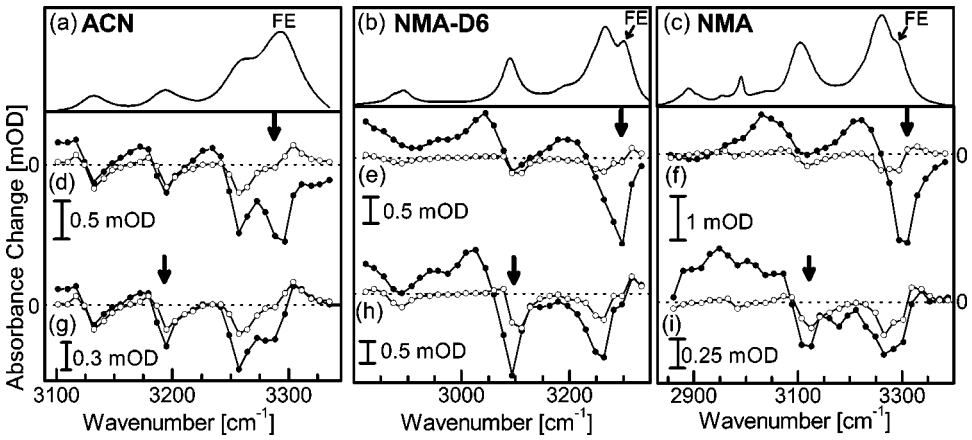

FIG. 9. Sections of the NH band of (a) ACN, (b) NMA-D_6, and (c) NMA. Pump-probe response after selective excitation of the high frequency band (d)–(f) and of the second satellite peaks (g)–(i) for 400 fs (•) and 4 ps (◦) delay times between the pump and the probe pulse. The arrows indicate the position of the narrow-band pump pulse. All three molecules show qualitatively similar responses.

In the case of NMA and NMA-D_6, we were unable to observe beatings in the pump-probe signal. Since the splitting between the satellite states is about three times larger in NMA than in ACN [Figs. 2(c) and 2(d)], one expects that the frequency of the corresponding phonon modes is larger by about the same factor. Part of this difference might be explained by the smaller mass of NMA. Such a high frequency mode would be at the detection limit of our setup, which is determined by the IR pulses duration. Technical improvements, i.e., pulse compression techniques, might make it possible to uncover these modes in the future. It could be also possible that the lifetime of the phonons in NMA are significantly shorter than in ACN, as suggested by the broader Raman lines,[32] and that they are thus much harder to detect.

C. Frequency-selective excitation of the NH band

Crystalline ACN. In this section we selectively excite the main peak and the satellite peaks in the NH spectrum of ACN and NMA using narrow-band, tunable pump pulses (see Fig. 9). For ACN we have discussed this response in detail in a previous publication.[21] In brief, the response of the main peak, which is, in the case of ACN, the peak with the strongest intensity and the highest frequency, differs distinctively from that of the satellite peaks. Immediately after pumping the main peak [Fig. 9(d)], a strong bleach and stimulated emission signal is observed at the position of that peak. The signal recovers on a 400 fs$\pm$100 fs time scale, representing the lifetime of this state [see Fig. 7(a)]. Simultaneously, the population is transferred into lower-lying states, giving rise to negative signals at the position of the satellite bands. On the other hand, when exciting one of the satellite states directly [Fig. 9(g)], we observe negative signals at the position of all satellite peaks, but not at the position of the main band. In Ref. 21, we have interpreted this response as a direct manifestation of self-trapping. Pumping the main peak transfers population on an ultrafast 400 fs time scale into the satellite peaks, i.e., into the self-trapped states. The main peak shows a small Davydov splitting [Fig. 2(e)], which indicates that the band corresponds to a delocalized state, i.e., a free-exciton state. On the other hand, when pumping the self-trapped states directly, no back population of the free exciton state is observed.

Crystalline NMA and NMA-D_6. Interestingly, a similar response is also found in the pump-probe response of NMA and NMA-D_6, except that the free exciton no longer relates to the peak with the highest intensity, but to a shoulder on the high-frequency side (marked with "FE" in Figs. 2 and 9). Also, this band shows a Davydov splitting between the parallel and perpendicular spectrum [Fig. 2(h)]. Both in NMA and in NMA-D_6, a bleach of all bands is observed when the pump pulse is resonant with that shoulder, and the signal at the shoulder band decays on an ultrafast timescale comparable to the free exciton band in ACN (Fig. 7). A direct excitation of one of the satellite peaks, on the other hand, reveals negative signals for all bands except for that shoulder, just as an excitation of a self-trapped state in ACN. In conclusion, we observed also in NMA two different types of states, whose nonlinear response matches the free-exciton and the self-trapped state in ACN.

IV. DISCUSSION

In the present paper, we compare the spectral response of two commonly used model systems for peptides: crystalline ACN and crystalline NMA, as well as their carbon-deuterated derivates. While the absorption spectra of these compounds, as well as their pump-probe signals, differ in detail, they exhibit striking similarities, which shall be summarized again.

(1) The amide I bands of ACN and NMA both contain a temperature-dependent "anomalous" band; however, the separation from the main peak is about three times smaller in NMA (Fig. 3).

(2) The NH bands of ACN and NMA are both accompanied by a sequence of equidistant satellite peaks towards lower frequencies (Fig. 2). The spacing between these satellite peaks is about three times larger in NMA.

(3) The narrow-band pump-probe signals of the NH band of ACN and NMA reveal similar responses (Fig. 9). In particular, two different types of states can be identified in both cases, one being the free-exciton (the highest frequency band) and the other being the self-trapped states (the satellite peaks).

(4) Quantum beats are observed in the broadband pump-probe signal of both ACN and ACN-D_8. The temperature dependence of the quantum beats substantiated our previous

result that they relate to the phonons which mediate self-trapping.

In the case of crystalline ACN, it is now well established that the signatures in the CO and NH spectra are a manifestation of vibrational self-trapping. The spectral appearance of ACN is very special, with probably the clearest manifestation of vibrational self-trapping. Nevertheless, we find striking similarities in the spectral response of crystalline NMA, from which we conclude that the mechanism behind the complicated band shapes are the same in both cases. Hence, one might speculate that self-trapping is not a unique property of crystalline ACN, but a general phenomenon in hydrogen-bonded crystals. This is indeed expected since the theory behind vibrational self-trapping is rather general. It essentially only depends on two coupling parameters, the exciton coupling and the exciton-phonon coupling, which are expected to be similar in crystals of comparable structure.

Also the NH absorption band of polypetides and proteins contains sidebands, which have been discussed in many early papers. [29,38–42] In 1951, Ambrose and Elliott already suggested that the sidebands of the NH stretching frequencies in polyamides, polypeptides, proteins, and ACN are caused by a system of coupled hydrogen-bonded NH oscillators.[38] Bradbury and Elliott proposed that the NH band in NMA is a combination between a genuine NH stretching vibration and a low-frequency vibration of the hydrogen bond (i.e., the same mechanism as the one discussed here, although the authors did not use the term "vibrational self-trapping").[29]

Nevertheless, it is now considered to be textbook knowledge that the doublet found for the NH band in polypetides and proteins (i.e., the main peak at 3300 cm^{-1} and the first satellite peak at 3100 cm^{-1}) is the result of a Fermi resonance between the NH mode and an overtone of the amide II vibration.[39,40,42,43] One generally refers to these two bands as the amide *A* and amide *B* band. The Fermi resonance assignment predominantly goes back to work by Krimm *et al.*, who have performed normal mode calculations for various polypeptides based on empirical force fields.[44–47] These works tried to assign in detail the overtone and/or combination mode which is supposed to be involved in the Fermi resonance. As a criterion for this assignment, the frequency and symmetry species of the modes have been used, but, of course, little was known about anharmonic couplings, i.e., the third ingredient needed to obtain a Fermi resonance. In the case of a β sheet, two different symmetry species of amide II must couple to form the amide *B* band, while in case of an α helix, an overtone of only one amide II species is necessary.[44,45] In different β sheets, such as β-poly(L-glycine) and β-poly(L-alanylglycine), the amide *B* mode originates from different pairs of symmetry species.[45] Furthermore, studies on N-deuterated β polypeptides[46] used a three-level Fermi resonance to explain the experimentally observed amide *A* and *B* bands. All these calculations agree well with the experimental data and explain temperature-dependent shifts in the spectra. Nevertheless, it seems striking that *different* sets of modes are required to explain the *uniform* appearance of the amide *B* mode in various secondary structure motifs. It is not surprising that one can always find a combination of modes that fits the Fermi resonance picture, given the huge density of states in a molecule as large as a polypeptide.

Also in the case of NMA, the two intense peaks in the NH band (3100 and 3250 cm^{-1}) have been previously assigned to a Fermi resonance and were referred to as amide *A* and *B* modes.[39,40] The remaining bands in the sequence of satellite peaks (2650 and 2900 cm^{-1}) have been interpreted as Fermi resonances with the overtone of the amide III band and a combination mode of amide II + amide III, respectively.[41] Nevertheless, the Fermi resonance interpretation for the NH band in NMA has been questioned frequently in the literature.[29,32,48,49] Temperature-dependent infrared and Raman studies on NMA and various isotopic species showed that a simple Fermi interpretation cannot account for the two intense peaks in NMA. The present work provides strong evidence that vibrational self-trapping at least contributes to the peculiar line shape of NMA.

The Fermi resonance picture completely ignores the effect of hydrogen bonding on the NH mode. It is well known that the NH mode in hydrogen-bonded systems strongly couples to low frequency vibrations of the hydrogen bond itself.[50,51] This coupling, which is a result of the highly anharmonic hydrogen-bond potential, leads to a redsshift of the absorption band, an intensity increase, and a band broadening accompanied by a peculiar band shape with a rich substructure. Both coupling mechanisms, Fermi resonance and coupling to low frequency modes, can coexist in a hydrogen-bonded system. Recent theoretical studies have taken both coupling mechanisms into account to describe the spectra of hydrogen-bonded vibrational modes.[52,53] The simulations result in band shapes that depend strongly on the relative strength of the two couplings and range from a typical Fermi resonance doublet to complex substructures with regularly spaced sidebands.

V. CONCLUSION

NMA is considered to be the prototype molecule to study vibrational spectra of peptides, with an obvious extension to polypeptides and proteins. Our study suggests that the previous assignment of the amide *A* and amide *B* bands in NMA solely to a Fermi resonance is clearly not sufficient, and that exciton-phonon coupling, leading to vibrational self-trapping, plays an important additional role. However, when the coupling mechanism in the prototype molecule needs to be reevaluated, then the interpretation of the amide *A* and *B* modes in polypeptides and proteins may be questioned as well. Clearly a careful analysis, which considers hydrogen bonding coupling to low frequency modes and Fermi resonances, is needed to understand the complex NH band shape in polypeptides. We are currently performing similar experiments on a real α helix which also yield strong evidence for vibrational self-trapping of the NH band.[54]

ACKNOWLEDGMENT

The work was supported by the Swiss National Science Foundation under Contract No. 2100-067573/1.

*Email address: jedler@pci.unizh.ch
†Email address: phamm@pci.unizh.ch

[1] A. S. Davydov, J. Theor. Biol. **66**, 379 (1977).
[2] H. Fröhlich, Adv. Phys. **3**, 325 (1954).
[3] A. C. Scott, Phys. Rep. **217**, 1 (1992).
[4] H. Torii and M. Tasumi J. Chem. Phys. **96**, 3379 (1992).
[5] S. Krimm and J. Bandekar, Adv. Protein Chem. **38**, 181 (1986).
[6] D. M. Alexander and J. A. Krumhansel, Phys. Rev. B **33**, 7172 (1986).
[7] H. Torii, T. Tatsumi, and M. Tasumi, Mikrochim. Acta **14**, 531 (1997).
[8] G. Careri, U. Buontempo, F. Carta, E. Gratton, and A. C. Scott, Phys. Rev. Lett. **51**, 304 (1983).
[9] N. B. Abbot and A. Eliott, Proc. R. Soc. London, Ser. A **234A**, 247 (1956).
[10] A. Scott, E. Gratton, E. Shyamsunder, and G. Careri, Phys. Rev. B **32**, 5551 (1985).
[11] C. B. Eilbeck, P. S. Lomdahl, and A. C. Scott, Phys. Rev. B **30**, 4703 (1984).
[12] J. Sauvajol, G. D. Nunzio, R. Almairac, J. Moret, and M. Barthés, Solid State Commun. **77**, 199 (1991).
[13] C. T. Johnston and B. I. Swanson, Chem. Phys. Lett. **114**, 547 (1985).
[14] G. B. Blanchet and C. R. Fincher, Jr., Phys. Rev. Lett. **54**, 1310 (1985).
[15] A. Spire, M. Barthes, H. Kellouai, and G. D. Nunzio, Physica D **137**, 392 (2000).
[16] M. Barthes, H. Kellouai, G. Page, J. Moret, S. W. Johnson, and J. Eckert, Physica D **68**, 45 (1993).
[17] M. Barthes, R. Almairac, J.-L. Sauvajol, and J. Moret, Phys. Rev. B **43**, 5223 (1991).
[18] G. Careri, U. Buontempo, F. Galluzzi, A. C. Scott, E. Gratton, and E. Shyamsunder, Phys. Rev. B **30**, 4689 (1984).
[19] H. J. Wassermann, R. R. Ryan, and S. P. Layne, Acta Crystallogr., Sect. C: Cryst. Struct. Commun. **C41**, 783 (1985).
[20] D. M. Alexander, Phys. Rev. Lett. **54**, 138 (1985).
[21] J. Edler, P. Hamm, and A. C. Scott, Phys. Rev. Lett. **88**, 067403 (2002).
[22] J. Edler and P. Hamm, J. Chem. Phys. **117**, 2415 (2002).
[23] J. Edler and P. Hamm, J. Chem. Phys. **119**, 2709 (2003).
[24] M. Barthes, J. Mol. Liq. **41**, 143 (1989).
[25] C. J. Brown and D. E. C. Corbridge, Acta Crystallogr. **7**, 711 (1954).
[26] J. L. Katz and B. Post, Acta Crystallogr. **13**, 624 (1960).
[27] P. Hamm, R. A. Kaindel, and J. Stenger, Opt. Lett. **25**, 1798 (2000).
[28] J. Eckert, M. Barthes, W. T. Klooster, A. Albinati, R. Aznar, and T. F. Koetzle, J. Phys. Chem. B **105**, 19 (2001).
[29] E. M. Bradbury and A. Elliott, Spectrochim. Acta **19**, 995 (1963).
[30] F. Fillaux, Chem. Phys. **62**, 287 (1981).
[31] M. Barthes, H. N. Bordallo, J. Eckert, O. Maurus, G. de Nunzio, and J. Léon, J. Phys. Chem. B **102**, 6177 (1998).
[32] W. A. Herrebout, K. Clou, and H. O. Desseyn, J. Phys. Chem. A **105**, 4865 (2001).
[33] G. Careri, E. Gratton, and E. Shyamsunder Phys. Rev. A **37**, 4048 (1988).
[34] C. T. Johnston, S. F. Agnew, J. Eckert, L. H. Jones, B. I. Swanson, and C. J. Unkefer, J. Phys. Chem. **95**, 5281 (1991).
[35] V. P. Gerasimov, Opt. Spektrosk. **43**, 705 (1977).
[36] M. Sakai, N. Kuroda, and Y. Nishina, Phys. Rev. B **47**, 150 (1993).
[37] J. Sauvajol, R. Almairac, J. Moret, M. Barthes, and J. Ribet, J. Raman Spectrosc. **20**, 517 (1989).
[38] E. J. Ambrose and A. Elliott, Proc. R. Soc. London, Ser. A **205**, 47 (1951).
[39] T. Miyazawa, J. Mol. Spectrosc. **4**, 168 (1960).
[40] M. Beer, H. B. Kessler, and G. B. B. Sutherland, J. Chem. Phys. **29**, 1097 (1958).
[41] H. Pivcová, B. Schneider, and J. Štokr, Collect. Czech. Chem. Commun. **30**, 2215 (1965).
[42] T. Miyazawa, in *Poly α Amino Acids*, edited by G. D. Fasman (Marcel Dekker, New York, 1967), pp. 69–103.
[43] R. M. Badger and A. D. E. Oullin, J. Chem. Phys. **22**, 1142 (1954).
[44] W. H. Moore and S. Krimm, Biopolymers **15**, 2439 (1976).
[45] W. H. Moore and S. Krimm, Biopolymers **15**, 2465 (1976).
[46] S. Krimm and A. M. Dwivedi, J. Raman Spectrosc. **12**, 133 (1982).
[47] S.-H. Lee, N. G. Mirkin, and S. Krimm, Biopolymers **49**, 195 (1999).
[48] G. Dellepiane, S. Abbate, P. Bosi, and G. Zerbi, J. Chem. Phys. **73**, 1040 (1980).
[49] F. Fillaux and M. Baron, Chem. Phys. **62**, 275 (1981).
[50] *Theoretical Treatment of Hydrogen Bonding*, edited by D. Hadži (Wiley, New York, 1997).
[51] O. Henri-Rousseau and P. Blaise Adv. Chem. Phys. **103**, 1 (1998).
[52] H. Ratajczak and A. M. Yaremko, Chem. Phys. Lett. **314**, 122 (1999).
[53] K. Belhayara, D. Chamma, and O. Henri-Rousseau, J. Mol. Struct. **648**, 93 (2003).
[54] J. Edler, R. Pfister, V. Pouthier, C. Falvo, and P. Hamm (unpublished).